HYDROLOGICAL PROCESSES
Hydrol. Process. **25**, 80–89 (2011)
Published online 29 July 2010 in Wiley Online Library
(wileyonlinelibrary.com) DOI: 10.1002/hyp.7821

Effects of land cover change on flood peak discharges and runoff volumes: model estimates for the Nyando River Basin, Kenya

L. O. Olang[1]* and J. Fürst[2]

[1] *Department of Agricultural Engineering, Egerton University, P. O. Box 536, Njoro, Kenya*
[2] *Institute of Water Management, Hydrology and Hydraulic Engineering (IWHW), University of Natural Resources and Applied Life Sciences, Muthgasse 18, Vienna, Austria*

Abstract:

The impacts of historical land cover changes witnessed between 1973 and 2000 on the hydrologic response of the Nyando River Basin were investigated. The land cover changes were obtained through consistent classifications of selected Landsat satellite images. Their effects on runoff peak discharges and volumes were subsequently assessed using selected hydrologic models for runoff generation and routing available within the HEC-HMS. Physically based parameters of the models were estimated from the land cover change maps together with a digital elevation model and soil datasets of the basin. Observed storm events for the simulation were selected and their interpolated spatial distributions obtained using the univariate ordinary Kriging procedure. The simulated flows from the 14 sub-catchments were routed downstream afterwards to obtain the accrued effects in the entire river basin. Model results obtained generally revealed significant and varying increases in the runoff peak discharges and volumes within the basin. In the upstream sub-catchments with higher rates of deforestation, increases between 30 and 47% were observed in the peak discharge. In the entire basin, however, the flood peak discharges and volumes increased by at least 16 and 10% respectively during the entire study period. The study successfully outlined the hydrological consequences of the eminent land cover changes and hence the need for sustainable land use and catchment management strategies. Copyright © 2010 John Wiley & Sons, Ltd.

KEY WORDS land cover; modelling; runoff; peak discharge; flood volume; Nyando Basin

Received 21 October 2009; Accepted 14 June 2010

INTRODUCTION

The need for environmental sustainability through proper resource management has prompted accurate and timely monitoring of land cover changes and their interactions within the immediate environments to provide vital information for decision making. In Kenya, land cover degradation arises primarily due to uncontrolled activities from the up-surging human population. Coupled with lack of appropriate land- and water-management strategies, this degradation is considered to amplify hydrological processes related to surface runoff, soil erosion and sedimentation (Kundu *et al*., 2008; Githui *et al*., 2009). In the flood-prone Nyando River Basin, the headwater catchments fundamental for the regeneration of the water resources have been drastically depleted in the recent past. More questions are thus being raised about the possible effects of this degradation on flood runoff characteristics. Like many rural river basins in the developing countries, however, a major impediment towards hydrological investigations in the Nyando Basin is a lack of reliable datasets (Corey *et al*., 2007). Most of the land cover datasets for the basin have very coarse spatial resolution and carry little information on the temporal changes (Awiti *et al*., 2002; Olang, 2009). There is also a deficiency of reliable hydrological data for understanding the interactions within the complex catchment system (Beasley *et al*., 1980). The availability of global spatial datasets, consequent of the recent advances in remote sensing and geographic information system (GIS) techniques have provided the possibility to quantify spatially distributed hydrological processes in regions with data scarcity (Moore *et al*., 1991; Carpenter *et al*., 1999; Coppin *et al*., 2004). Pertinent physically based catchment properties can be estimated from global digital topographic and soil datasets. Consequently, several computer-based hydrological models that exploit these provisions have been developed and successfully employed for hydrological analyses (Andersen *et al*., 2001; Miller *et al*., 2002; Legesse *et al*., 2003).

Physically based hydrological models attempt to relate the model parameters to observable land surface characteristics. As a result, such models are extensively utilized for studies of the effects of land cover changes on surface and sub-surface hydrologic processes (Xu and Singh, 2004; McColl and Aggett, 2007; Saghafian *et al*., 2007). In hydrological simulation studies, the selection of appropriate spatial and temporal scales to represent a

* Correspondence to: L. O. Olang, Faculty of Engineering and Technology, Department of Agricultural Engineering, Egerton University, P. O. Box 536, Njoro, Kenya. E-mail: olanglk@yahoo.com

hydrological variable of consideration is essential to capture the relevant random and non-random patterns (Grayson and Blöschl, 2000; Cerdan *et al*., 2004; Doll *et al*., 2008). A careful evaluation of the hydrological attribute*s* versus the quality of the existing datasets is hence important. While distributed models tend to capture more hydrological information than the lumped models (Refsgaard and Knudsen, 1996; Reed *et al*., 2004), their application within most of the data-constrained areas, however, is limited by their vast data demands (Onyando *et al*., 2005; Corey *et al*., 2007). Moreover, most of the conventional hydrological models were developed in regions with different hydro-climatic characteristics. Their application elsewhere, therefore, requires adaption to the local data constraints, the existing landscape patterns and characteristics of the hydrological processes (Gumbricht *et al*., 1997; Mutua and Klik, 2007). In this contribution, therefore, the objectives of the study were as follows: (1) To parameterize the selected hydrological models using remotely sensed land cover datasets in combination with other available spatial datasets. The land cover changes were obtained through a comprehensive change detection strategy carried out by processing selected Landsat satellite images. (2) To apply the hydrological models to simulate the possible effects of the detected land cover changes on peak discharges and runoff volumes during flood events of the study area.

THE STUDY AREA

The Nyando River Basin covers an area of about 3550 km^2. It is located in western Kenya, in the scarps of the Kavirondo Gulf, between 0°25′S and 0°10′N and 34°50′ E and 35°50′E. The climate is largely influenced by the inter-tropical convergence zone (ITCZ), modified by local orographic effects. In terms of rainfall seasonality, the basin is classified as bimodal, having a long rainy season predominantly between the months of April and June, and a short rainy season between September and December. The average annual rainfall depth is about 1300 mm on a normal year devoid of extreme rainfall events due to climatic variations such as the El Niño southern oscillation (ENSO). Soils with high content of silt and clay consequent of *Ferrasols, Nitisols, Cambisols* and *Acricsols* are predominant in the upland areas. The lowland floodplains are dominated by *Luvisol, Vertisol, Planosol, Cambisol* and *Solonetz* soil types from the Holocene sedimentary deposits and occurring in saline and sodic phases (Andriesse and Van der Pouw, 1985). The basin is drained by the Nyando River with a total length of about 170 km. The river has two major tributaries originating from the Nandi Hills in the northern part at altitudes of about 2600 m *a.m.s.l* and Londiani Hills in eastern sides at altitudes of about 3000 m *a.m.s.l.* The Nyando River finally drains into the transboundary Lake Victoria situated at about 1100 m *a.m.s.l.* (Figure 1).

MATERIALS AND METHODS

The major building blocks of the study were grouped into spatial data processing and hydrological modelling. Spatial data processing largely revolved around the land cover change detection and geographical data processing. Hydrological modelling was then applied to study the impacts of land cover change on flood characteristics. Figure 2 is a schematic illustration of the general methodology of the study.

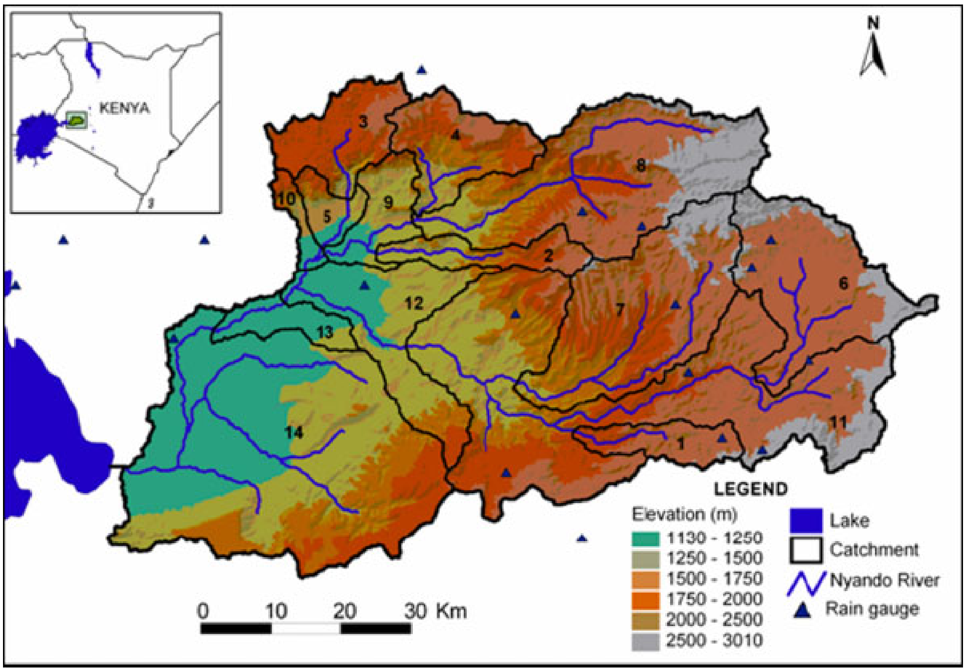

Figure 1. The study area showing the sub-catchments, the elevations and the rain gauge stations of the Nyando Basin

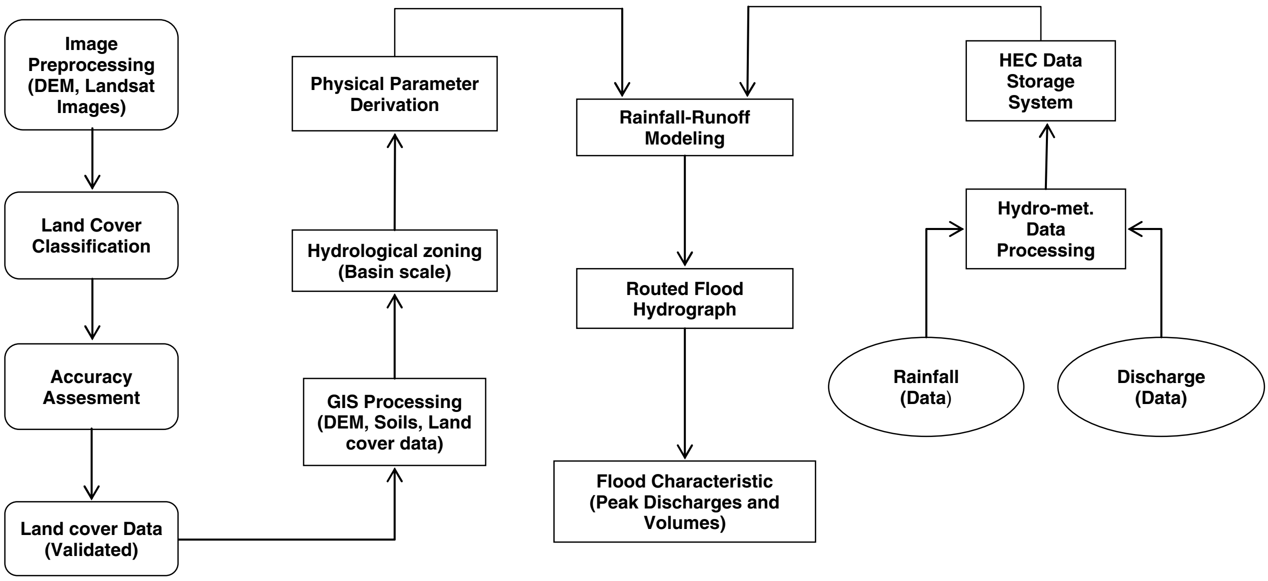

Figure 2. Methodological framework of the study

Spatial datasets and processing

Changes in the historical land cover states were quantified through a comprehensive land cover change detection carried out in 2008 (Olang, 2009). This was achieved through classifications of selected satellite images for 1973 [Landsat Multispectral Scanner (MSS)], 1986 [Landsat Thematic Mapper (TM)] and 2000 [Landsat Enhanced Thematic Mapper *plus* (ETM+)] based on the major land cover classes including agricultural fields, forest, shrubland, wetland and water. To obtain spatially representative and consistent land cover datasets, a per-pixel classification of the images was applied. The accuracies of the derived maps were assessed on the basis of standard procedures with the help of the FAO-Africover dataset and ground-based information (Di Gregorio and Jansen, 1998; Congalton and Green, 1999; Yuan *et al.*, 2005; Baldyga *et al.*, 2007; Rambaldi *et al.*, 2007). The spatial distribution of the validated land cover classes is summarized in Figure 3.

Topological and morphometric characteristics of the basin were derived from the global digital elevation model (DEM) developed by the Shuttle Radar Topographic Mission (SRTM) (Reuter *et al.*, 2007). Four tiles encompassing the study area were acquired and resampled to a nominal pixel resolution of 80 m in consistency with the land cover datasets using bilinear interpolation. The dataset was then hydrologically corrected through sink removal and a DEM burn-in procedure (Martz and Garbrecht, 1998; Callow *et al.*, 2006). The sub-catchments and their attributes were derived using standard procedures based on the D8 (eight-pour-point algorithm) concept of flow directions and accumulation (Moore *et al.*, 1991; Burrough and McDonell, 1998). In order to use the land cover change maps together with other spatial datasets for subsequent hydrological analyses, a 7×7 majority filter was used to eliminate small, isolated landcover units. The images were later on converted into vector coverages in conformity with the model demands and used to derive the required land cover change statistics. A digital soil map for Kenya, at a scale of 1 : 1 million, was acquired from the Global Environment Facility Soil Organic Carbon database and used to

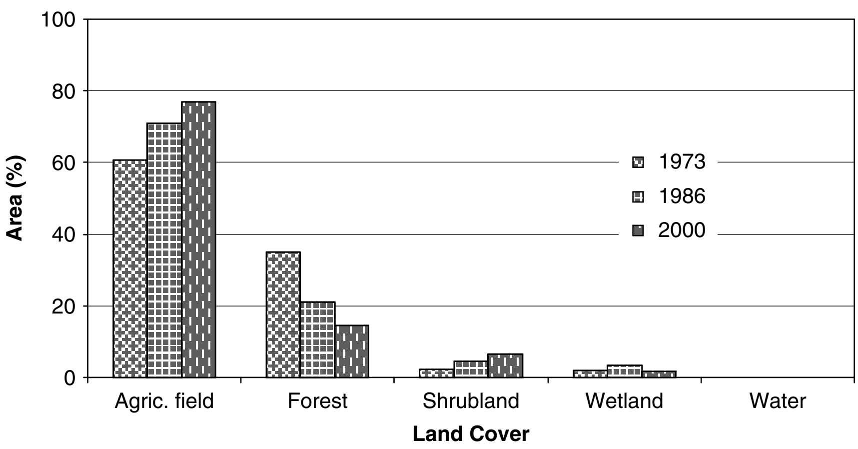

Figure 3. Distributions of the land cover classes

derive the major hydrological soil groups (HSG) with the help of FAO/UNESCO revised manual for soil maps of the world (FAO-UNESCO, 1998; Batjes and Gicheru, 2004). The other relevant spatial datasets processed for specific applications included the approximate areas of the local administrative centres and roads, used to estimate the impervious zones within the sub-catchments (Olang, 2009).

Hydro-meteorological data

Daily rainfall data from 18 pluviometric stations were obtained from the Kenya Meteorological Department (KMD). Daily discharge data from 13 stream gauges were collated from the Ministry of Water and Irrigation, Kenya. A comparison of the acquired rainfall and runoff data on a common graphical plot revealed many uncertainties in the recordings. The runoff data, in particular, exhibited poor recordings and large data gaps especially during flood events. Moreover, an exemplary review of the stage-discharge curves used for conversion of the recorded river stages into discharge revealed them to be highly unreliable. These shortcomings limited the ability to calibrate the hydrological model during the periods of the three land cover states. Nevertheless, the acquired runoff data were deemed, at least, sufficient for approximating initial baseflow discharges for the selected periods. The geographical locations of the stream gauges were also considered to be helpful in defining spatial units for the modelling exercise. Some of the characteristics of the acquired stream flow data, sorted out according to their representative areas from upstream to downstream, are provided in Table I.

Since the acquired stream flow data could not be used for a reliable model calibration and validation procedure, only plausibility checks of the simulated results were possible (Wagener, 2003; Refsgaard and Henriksen, 2004). This was done through visual comparison if the simulated runoffs fell within the range of the available discharge records for the respective sub-catchments. Runoff coefficients, defined by the simple ratio of the simulated runoff depths to the rainfall amounts, coupled with expert judgments were also used to judge the simulated estimates (Onyando, 2000; Merz and Blöschl, 2007).

A physically based lumped modelling approach involving rigorous use of GIS-based techniques to derive the model parameters was adopted to simulate storm events. A number of observed storm events were selected, and their interpolated spatial rainfall distributions within the sub-catchments subsequently obtained using the univariate ordinary Kriging procedure (Cressie, 1993). To further assess the unique response of the sub-catchments due to the mapped changes, synthetic storm events of varying magnitudes were proposed on the basis of the rainfall characteristics of the basin. The storms were also assumed to have the same durations corresponding, approximately, to the times of concentration of the sub-catchments. The selected observed and synthetic storm events were subsequently stored in the Hydrologic Engineering Center (HEC) Data Storage System Visual utility engine (DSSVue) for the simulation (USACE, 2000a). The characteristics of the selected observed storm events used for illustration in this paper are provided in Table II.

HEC-HMS model and parameterization

A hydrological model, whose parameters are sensitive to the detected land cover changes, was required. The use of a fully distributed physically based approach to achieve this was, however, constrained by the availability and quality of the required data. Therefore, a conceptual lumped model whose parameters could be largely derived from the land cover change maps was considered to be an appropriate approach. (Xu and Singh, 2004; Bahremand *et al*., 2006). The HEC Hydrological Modelling System (HMS) provided a sufficient and easily accessible platform to achieve this (USACE, 2000a). The modelling system generally offers a variety of options for simulating various hydrological processes while providing flexibility in representing the hydrological processes at lumped or distributed scales, on event or continuous basis. Several studies have hence utilized the modelling software

Table I. Major statistics of stream flow data for the sub-catchments

ID	Sub-catchment	Stream gauge	Spatial location		Total area upstream	Missing data	Maximum discharge
			Latitude (°)	Longitude (°)	(km^2)	(%)	(m^3/s)
1	Tugunon	1GC04	−0·25	35·41	73·7	7	50
2	Mbogo	1GB06	−0·06	35·14	77·2	60	4
3	Kapchure1	1GB07	−0·01	35·10	130·7	15	14
4	Ainapsiwa	1GB11	−0·03	35·18	147·7	10	75
5	Kapchure2	1GB10	−0·06	35·07	176·0	26	31
6	Masaita	1GC05	−0·19	35·54	285·6	12	57
7	Namuting	1GG01	−0·20	35·34	365·3	5	62
8	Ainamotua2	1GB05	−0·03	35·18	594·1	11	75
9	Ainamotua3	1GB09	−0·07	35·08	753·3	9	25
10	Ainamotua1	1GB03	−0·07	35·06	957·7	19	539
11	Nyando3	1GD07	−0·16	35·16	1472·1	11	306
12	Nyando2	1GD04	−0·10	35·04	2650·4	40	320
13	Nyando1	1GD03	−0·13	34·96	2711·7	8	360
14	Lower SB	Outlet	—	—	3543·5	—	—

Table II. Selected observed storm events

Date	Highest gauge measurement (mm)	Approximate rainfall duration (h)	Major spatial distribution of the event	Areal rainfall for the basin (mm)
3 January 1998	66	5	South eastern	18
2 May 1972	72	5	Upland headwaters	27
8 April 1974	92	6	Mid to lowlands	41

for various hydrological applications (e.g. Cunderlik and Simonovic, 2007; McColl and Aggett, 2007; Saghafian *et al*., 2007).

For this study, the Natural Resource Conservation Service-Curve Number (NRCS-CN) model, Clark's Unit Hydrograph model, exponential recession baseflow model and Muskinghum–Cunge flow routing model were selected. The model elements for the basin were derived using Geo-HMS, a GIS extension to support the HEC-HMS (USACE, 2000b). The NRCS-CN model was used for generating runoff volumes (USACE, 1994). The model approximates runoff volumes using the physically based dimensionless curve number (CN) parameter, which could be easily derived from the land cover maps for 1973, 1986 and 2000. The application of this model within HEC-HMS requires specification of the CN, initial abstraction and percentage of impervious area (Olang, 2009). The general procedure used to determine the composite CN parameter is provided in Figure 4.

A look-up table for retrieving CN estimates was developed for normal moisture conditions (AMC II) with the help of standard tables (Chow *et al*., 1988). Initial estimates for agricultural land use were adopted and later re-adjusted to wet moisture conditions (AMC III) prevalent during storm events. The initial abstractions were assumed to be 20% of the maximum potential retention of the soils (USACE, 2000a). Impervious areas, assumed to be largely due to the local administrative centres and roads, were derived from the acquired GIS layer representing their approximate areas within the regions. Transformation of the generated runoffs into corresponding hydrographs was achieved using Clark's UH concept (USACE, 1994). The application of Clark's UH requires the determination of the times of concentration and the storage coefficient. These parameters can be established from the physical catchment conditions based on procedures for the time lag (Soil Conservation Service, 1986) and the storage coefficients (Sabol, 1988). Since changes in the land cover affected these two parameters, the dependence between the runoff generation and transformation parameters was captured.

The exponential recession model was used to represent baseflow processes. The model requires estimation of the recession constant and the initial base flow. A similar approach outlined by Pilgrim and Cordery (1992) was used to estimate the recession constant based on the relative sizes of the sub-catchments. Ground water was assumed to be the main component of baseflow. Routing of the channel flow was performed using the Muskinghum–Cunge hydrologic model (Ponce, 1989; USACE, 2000a). Estimates for the depth and width of the river channel bottom and other flow characteristics were collated from the Lake Victoria Environmental Programme (LVEMP) in Kenya, supplemented by direct measurements where necessary. The length and slopes of the river reaches were derived from a DEM of the basin in the GIS. Other channel characteristics, including Manning's roughness coefficient at every reach of study, were estimated from field observations (Cowan, 1956). The stream channel characteristics were assumed to be time invariant from 1973 to 2000 and thus a plausible representation was considered to be sufficient in the context of this study, focusing on the effects of land cover change.

RESULTS AND DISCUSSION

Model Parameters

The land cover maps, together with the catchment properties and the hydrological soil groups, were used to estimate the main parameters of the selected models for the sub-catchments as shown in Table III. The parameters

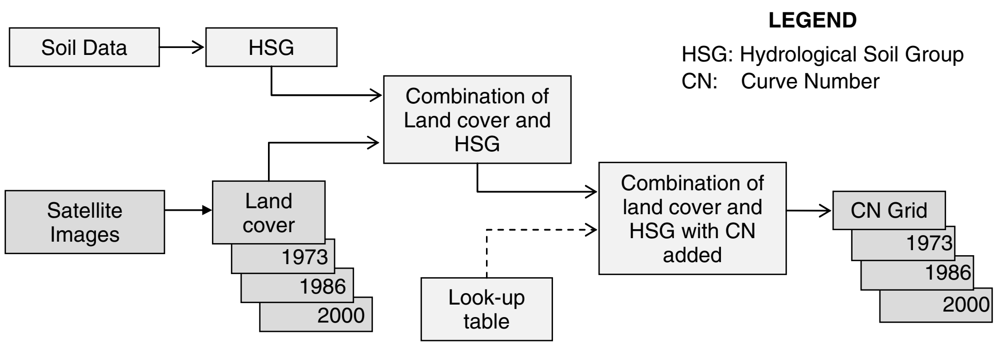

Figure 4. Procedure for derivation of the composite CN parameter

Table III. Estimated parameters of the rainfall-runoff models for the land cover states

ID	Mean curve number (CN)			Time of concentration (t_c)			Storage coefficient (R)		
	1973	1986	2000	1973	1986	2000	1973	1986	2000
	(%)	(%)	(%)	(h)	(h)	(h)	(h)	(h)	(h)
1	68·0	73·3	75·8	2·6	2·3	2·1	1·9	1·7	1·5
2	68·0	70·1	74·3	2·6	2·4	2·2	1·9	1·8	1·6
3	67·7	71·2	72·1	2·5	2·3	2·2	1·8	1·6	1·6
4	68·0	71·2	74·3	2·2	2·0	1·8	1·5	1·4	1·3
5	77·9	78·2	78·9	1·3	1·3	1·3	0·9	0·9	0·9
6	66·1	68·6	71·9	4·7	4·4	4·0	3·3	3·1	2·8
7	67·4	70·4	71·2	4·1	3·8	3·7	2·9	2·7	2·6
8	59·3	62·3	64·0	5·6	5·2	5·0	4·0	3·7	3·6
9	82·2	82·0	82·5	1·6	1·6	1·5	1·1	1·1	1·1
10	79·1	81·0	78·9	1·3	1·2	1·3	0·9	0·9	0·9
11	69·0	71·3	72·9	6·5	6·1	5·8	4·7	4·4	4·2
12	80·8	81·2	82·5	3·8	3·8	3·6	2·7	2·7	2·6
13	85·7	86·0	87·3	3·8	3·7	3·6	2·7	2·7	2·6
14	78·1	79·1	80·1	5·9	5·7	5·5	4·1	4·0	3·9

have been sorted on the basis of the sub-catchment ID as mapped in Figure 1.

From the derived composite CN values, different regions in the basin were noted to have significantly changed. Sub-catchment Nos 9, 10, 12 and 13 generally produced the largest values of the CN parameter. A decrease in the CN value was, however, noted in sub-catchment No. 10 between 1986 and 2000, perhaps due to seasonal fluctuations between agriculture and grassland land cover classes. In terms of changes in the CN parameter relative to 1973, the largest increases were noted in the upstream sub-catchments Nos 1, 2, 3 and 4, where the highest rates of deforestation occurred over the years. Sub-catchment No. 11 exhibited the largest times of concentration and the storage coefficients due to its longer shape and relative size. The smallest value of the runoff transformation parameters was noted in sub-catchment No. 10, which is the smallest (28 km^2).

Simulated flood peak discharges and volumes

Using the model parameters, the arising local flood flows from each sub-catchment were simulated. The impact of the land cover changes were subsequently evaluated relative to the simulated values for 1973. First, the local flows from the sub-catchments were simulated using uniformly distributed synthetic storm events.

Synthetic storm events: Synthetic storm events with a spatially uniform distribution of 20, 40 and 60 mm were analysed. The rainfall depths correspond to crudely estimated return periods of 1–5 years. The storm duration was selected at 5 h, corresponding to the time of concentration of the larger sub-catchments. Rainfall depths for 1-h time intervals were uniformly assumed to be 20, 25, 35, 15 and 5% of the event depth, respectively. This pattern of aggregation is typical of the area as could be derived from the observed records. Table IV illustrates the simulated peak discharges and runoff depths produced by the sub-catchments from a 40-mm uniformly distributed synthetic storm event selected for illustration.

Table IV. Simulated peak discharges and runoff depth from the 40-mm synthetic storm event

ID	Sub-catchment	Runoff peak discharge (m^3/s)			Runoff depth (mm)		
		1973	1986	2000	1973	1986	2000
1	Tugunon	47·6	60·6	67·5	12·1	14·1	15·2
2	Mbogo	49·0	54·2	65·4	11·6	12·4	14·1
3	Kapchure1	84·1	98·5	102·4	11·0	12·2	12·6
4	Ainapsiwa	102·6	115·8	137·7	11·3	12·5	13·7
5	Kapchure2	56·3	57·2	59·2	17·1	17·3	17·6
6	Masaita	114·4	129·5	156·8	10·3	11·2	12·4
7	Namuting	169·0	196·6	204·7	10·8	11·9	12·2
8	Ainamotua2	122·0	145·5	158·8	8·1	9·0	9·5
9	Ainamotua3	112·4	113·6	115·2	22·6	22·7	22·9
10	Ainamotua1	41·6	45·0	42·1	11·6	11·7	11·8
11	Nyando3	251·7	286·3	310·0	11·2	12·1	12·8
12	Nyando2	181·7	185·9	198·4	21·2	21·5	22·3
13	Nyando1	68·7	69·8	74·3	23·4	23·6	24·7
14	Lower SB	426·4	451·9	483·3	16·2	16·8	17·4

Generally, the sub-catchments of the basin exhibited a consistent response to the land cover changes in the simulated results. In terms of the simulated peak discharges, sub-catchment No. 2, for instance, produced peak discharges of 49 m^3/s in 1973, 54 m^3/s in 1986 and 65 m^3/s in 2000. These values correspond to increases of 11, 23 and 34% for the periods 1973–1986, 1986–2000 and 1973–2000, respectively. In the same area, the runoff volumes increased by 7, 15 and 22%. The peak discharges produced by sub-catchment No. 6 corresponded to relative increases of 13, 25 and 38% over the same time intervals. In sub-catchment No. 14 located within the floodplains, the simulated peak discharges exhibited increases of about 6, 8 and 14%, respectively, within the three time intervals. Runoff volumes on the other hand increased by 9, 11 and 20% in sub-catchment No. 6, and by 5, 3 and 8% in the Lower SB.

Results obtained from the 60-mm synthetic rainfall event generally replicated the same trends, with sub-catchment No. 2, exhibiting simulated peak discharges of about 96 m^3/s in 1973, 105 m^3/s in 1986 and 125 m^3/s in 2000. These values were noted to almost double the values produced by the 40-mm synthetic storm event and corresponded to relative increases of 10, 20 and 30% for the three intervals of time. The relative increases in the runoff depths for the same sub-catchment were 7, 13 and 20%. In summary, an evaluation of the model results obtained from the synthetic storm events tested demonstrated that the relative changes in the peak discharges tended to decrease with increase in the rainfall amounts. This observation proved the possibility that the detected land cover changes did not have a very strong influence during large storm events. In sub-catchment No. 1, for instance, the relative changes in the peak discharge between 1973 and 2000 obtained from the 20, 40 and 60 mm synthetic storms were noted to be 45, 42 and 37% respectively. For the same storm events, sub-catchments Nos 7 and 3, located within the headwaters of the basin, also exhibited decreasing trends by 22, 21 and 19% and 24, 22 and 20% respectively, from the 20, 40 and 60 mm synthetic storms. Generally, the results also indicated that upstream sub-catchments characterized by the higher catchment slopes, and rates of land cover changes exhibited the highest relative changes in the peak discharge values in the range of 30–47%. The rainfall-runoff plots for an upstream sub-catchment (No. 1) and downstream sub-catchment (No. 14), selected for illustration purposes, are provided in Figures 5 and 6.

From Figures 5 and 6, a higher rise in peak discharge value consequent of the larger rate of land cover changes occurred between 1973 and 1986 in sub-catchment No. 1 located in the headwater area. This area generally produced the highest change effects in the basin due to its larger slopes and the increased deforestation. In the lower sub-catchment, the peak discharges increased almost by the same amount from 1973 to 1986 and from 1986 to 2000, respectively. This catchment is located within the flood plains of the basin largely dominated by agricultural and grassland land cover classes.

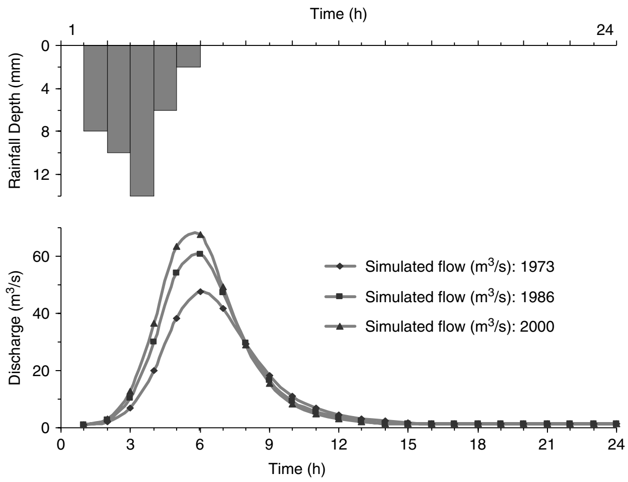

Figure 5. Rainfall-runoff plots for sub-catchment No. 1 (Tugunon)

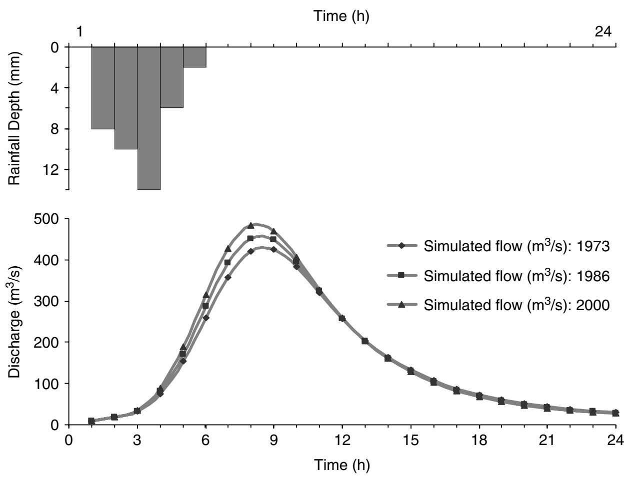

Figure 6. Rainfall-runoff plots for sub-catchment No. 14 (Lower SB)

Observed storm events: Table V illustrates the accumulated flood peak discharges and volumes obtained from the storm event observed on 3 January 1998. This flood event approximately conforms to a flood with a return period of about 2 years in the basin.

As a plausibility check, the simulated peak discharges for the land cover state of the year 2000 were compared with observed maximum discharges as listed in Table I. In general, simulated and observed peaks are rather similar, except in 1 GB03, 1 GB07 and 1 GB09. From the results, the entire basin witnessed peak discharges of 382, 425 and 459 m^3/s in 1973, 1986 and 2000 respectively. These represented an increase by 20% between 1973 and 2000, with 11% occurring in the first period of 1973 and 1986. The decreasing times to peak, with the same event taking approximately 1 h less to reach peak in 2000 than in 1973, were also noted. In terms of the flood volumes, this event produced flood volumes on the order of 17, 18 and 19 million m^3 in 1973, 1986 and 2000, representing increases of about 10% between 1973 and 2000 and about 6% between 1973 and 1986 when more land cover changes was witnessed in the basin. The results of the storm event for 2 May 1972 approximated a flood event with a return period of about 3 years. Peak discharges for 1973, 1986 and 2000 were noted to be 586, 658 and 708 m^3/s respectively. This represented increases by 12 and 9% for the periods of 1973–1986 and 1986–2000 respectively. Flood volumes on the other hand increased by 12% over the entire period of study. The simulated results from the 8-April-1974 storm event conformed approximately to a flood event with a return period of about 10 years. The results at the outlet, assumed to reflect the overall effects of the changes in the whole basin, indicated peak discharges of 1417, 1544 and 1645 m^3/s. These values suggested relative increases of 9, 7 and 16% for

Table V. Simulated flood peak discharges and volumes for 3 January 1998

ID	Gauging station	Runoff peak discharge (m^3/s)			Runoff volume ($\times 10^6$ m^3)		
		1973	1986	2000	1973	1986	2000
1	1GC04	48	64	74	0·89	1·04	1·12
2	1GB06	3	4	4	0·14	0·14	0·15
3	1GB07	25	30	31	0·43	0·48	0·49
4	1GB11	21	25	29	0·37	0·40	0·44
5	1GB10	31	38	40	0·70	0·74	0·76
6	1GC05	22	25	31	0·66	0·70	0·77
7	1GG01	71	84	89	1·75	1·92	1·97
8	1GB05	27	31	34	0·79	0·85	0·90
9	1GB09	44	49	55	1·56	1·62	1·68
10	1GB03	117	118	117	4·46	4·73	4·93
11	1GD07	231	273	302	7·06	7·73	8·17
12	1GD04	315	362	400	11·37	12·17	12·71
13	1GD03	329	374	411	12·67	13·48	14·04
14	Outlet	382	425	459	16·86	17·83	18·55

Table VI. Runoff coefficients and change in peak discharges in the sub-catchments (8 April 1974)

ID	Sub-catchment	Runoff coefficient (%)			Changes in peak discharge (% of Q_{max} 1973)		
		1973	1986	2000	1973–1986	1986–2000	1973–2000
1	Tugunon	29·2	34·0	36·8	28·9	18·4	47·4
2	Mbogo	34·0	36·1	40·9	9·4	21·9	31·3
3	Kapchure1	27·6	30·7	31·6	16·3	4·7	20·9
4	Ainapsiwa	31·4	34·6	38·1	14·8	15·7	30·4
5	Kapchure2	43·6	44·1	45·0	1·8	5·3	7·0
6	Masaita	18·0	19·5	21·6	17·5	25·0	42·5
7	Namuting	20·0	22·1	22·5	18·3	7·0	25·4
8	Ainamotua2	19·3	21·3	22·5	15·4	10·6	26·0
9	Ainamotua3	56·0	56·3	56·7	0·9	0·9	1·8
10	Ainamotua1	31·6	32·5	31·7	8·2	−6·1	2·0
11	Nyando3	28·4	30·6	32·4	13·8	9·5	23·3
12	Nyando2	54·8	55·4	57·5	2·6	7·7	10·3
13	Nyando1	65·2	65·9	66·7	1·5	5·8	7·3
14	Lower SB	45·0	46·6	48·1	6·3	6·0	12·3

1973–1986, 1986–2000 and 1973–2000 respectively. Table VI provides estimates of the runoff coefficients and changes in peak discharges obtained from the sub-catchments from this storm event. The changes have been defined relative to the simulated peak discharge (Q_{max}) for 1973.

From results, the sub-catchments Nos 1, 6, 2 and 4 located in the headwaters of the basin provided the highest relative changes in the peak discharges. All of these sub-catchments are located in the head waters of the basin. Apart from sub-catchment No. 1 with 47%, sub-catchments Nos 2 and 6 exhibited increases of about 31 and 43% respectively over the entire period (1973–2000). Generally, sub-catchments Nos 10 and 9 produced the lowest relative changes in the peak discharge over the entire period of 1973–2000. Between 1986 and 2000, however, sub-catchments No. 10 indicated a decrease in the peak discharge value due to the seasonal fluctuations of the land covers in this area as also reflected by the CN parameter between the years. Sub-catchments Nos 13, 9 and 12 provided the highest estimates of the runoff coefficients. These catchments are located in a region largely dominated by poorly drained soils with low infiltration characteristics. Onyando (2000), in his study of various humid catchments in Kenya, obtained runoff coefficient estimates in the range of 30–50% from storm events of about the same depths. A critical assessment of the simulated results from the three storm events revealed that bigger floods tended to attenuate quickly downstream within very short times to peak. Most of the storms tested over this observation revealed that the land cover changes tended to result in decreased times to peaks in the range of 1–3 h, with smaller storms exhibiting larger differences between the years than bigger storms. Figures 7 and 8 illustrate the flood hydrographs from the 8-April-1974 and 3-January-1998 storm events obtained at the final outlet assumed to represent the cumulated effects for the basin.

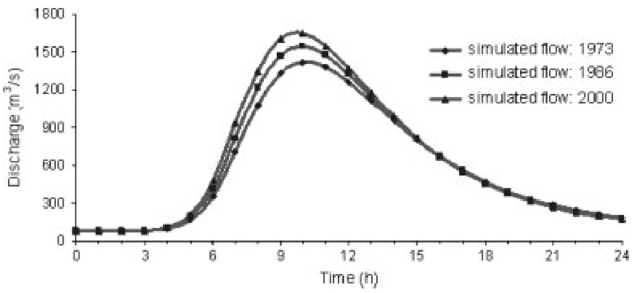

Figure 7. Simulated flood hydrograph for the basin (8 April 1974)

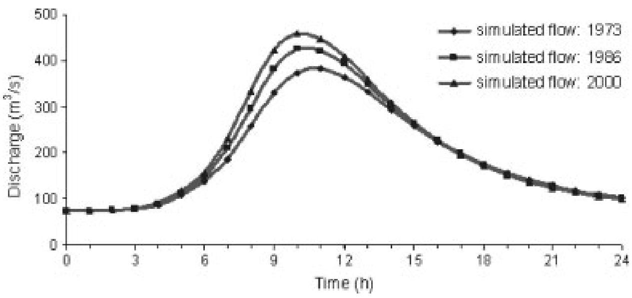

Figure 8. Simulated flood hydrograph for the basin (3 January 1998)

CONCLUSION AND RECOMMENDATION

This study successfully attempted to estimate the effects of historical land cover changes on flood peak discharges and volumes. The simulated results revealed that the detected land cover changes have increased peak discharges and flood runoff volumes within the sub-catchments. This effect was more severe within the upstream areas where higher rates of deforestation and agricultural expansion were rampant. However, the relative increases in the simulated peak discharges were noted to diminish with increasing rainfall amounts. This portended that the detected land cover changes did not have a strong influence during large storm events. Also, between the years of study, the flood times to peak indicated a decreasing trend with the increasing rainfall amounts, with smaller storms showing more variation in their times to peak than the bigger storms. Since changes in the land surface conditions can modify flow paths and storage capacities of catchments, this study emphasized the dependence of the model parameters that define these two processes. However, due to the inability to obtain morphological datasets for the three land cover states, the same parameters, derived from the acquired digital elevation model coupled with direct measurements, were used in routing the arising flows. Consequently, the possible effects of factors such as fluctuations in the river channel morphology likely to modify flood peak discharges and volumes could not be factored in. Moreover, the flow routing model used could not account for flood inundations normally prevalent within the floodplains. It is hence likely that the simulated peak discharges within the lower floodplains could be over-estimated.

Land use changes due to agricultural expansion remain one of the notable threats to the hydrology of most regions in Kenya. The study results of the Nyando Basin generally depict good trends in conformity with similar studies carried out in the region (Mati *et al.*, 2008; Githui *et al.*, 2009). The results, therefore, can be used to support policy options and catchment strategies geared towards flood runoff management. Nonetheless, further investigations in the study basin are inevitable. The application of a fully distributed modelling approach may help in detailing the flood characteristics within the vulnerable floodplains. Future studies aimed at investigating land cover/use scenarios best suited for minimizing flood flows in the basin should be investigated for catchment management purposes. Generally, considering data constraints in most of the catchments in Kenya, future hydrological studies can consider the application of other global spatial datasets such as soil moisture data derived from satellite sensors through various approaches independent of field observation or canopy biophysical measurements. Potential evapo-transpiration datasets from sources such as Moderate Resolution Imaging Spectro-radiometer (MODIS) and Advanced Very High Resolution Radiometer (AVHRR) remote sensors may also be imperative in this respect (De Jeu and Owe, 2003; Mallick *et al.*, 2007; Fisher *et al.*, 2008). It is also essential to explore procedures for quantifying modelling uncertainties within ungauged regions in order to understand the reliability of the simulated estimates.

ACKNOWLEDGEMENTS

The authors would like to acknowledge the financial support of the Austrian Development Cooperation through the Austrian Exchange Service (ÖAD). We are grateful to the relevant authorities at LVEMP, World Agroforestry Centre (ICRAF) and KMD in Kenya for providing the relevant data. We also acknowledge the technical support of Professor Laban Ogallo of IGAD Climate Prediction and Application Centre (ICPAC), Kenya. Many thanks to Professor Werner Schneider and Dr Thomas Bauer from the Institute of Surveying, Remote Sensing and Land Information (IVFL), University of Natural Resources and Applied Life Sciences (BOKU), Vienna, Austria for their technical support. To the anonymous reviewers, many thanks for your constructive comments and contributions.

REFERENCES

Andersen J, Refsgaard JC, Jensen KH. 2001. Distributed hydrological modeling of the Senegal River Basin—model construction and validation. *Journal of Hydrology* **247**: 200–214. DOI: 10.1016/S0022-1694(01)00384-5.

Andriesse W, Van der Pouw BJA. 1985. *Reconnaissance Soil Map of the Lake Basin Development Authority, Western Kenya (Scale 1 : 250 000)*, Netherlands Soil Survey Institute/Kenya Soil Survey: Wageningen, The Netherlands/Nairobi, Kenya.

Awiti AO, Walsh MG, Omuto C. 2002. Consequences of land cover change: land management and policy options. In *Reversing Environmental and Agricultural Decline in the Nyando River Basin*, Mungai D, Swallow B, Mburu J, Onyango L, Njui A (eds). ICRAF: Nairobi.

Bahremand A, De-Smedt F, Corluy J, Liu YB, Poorova J, Velcicka L, Kunikova E. 2006. WetSpa model application for assessing reforestation impacts on floods in Margecany-Hornad watershed, Slovakia. *Water Resources Management (Springer)* **21**(8): 1373–1391. DOI: 10.1007/s11269-006-9089-0.

Baldyga TJ, Miller NS, Driese LK, Gichaba NC. 2007. Assessing land cover change in Kenya's Mau Forest region using remotely sensed data. *African Journal of Ecology* **46**: 46–54. DOI: 10.1111/j.1365–2028.2007.00806.x.

Batjes NH, Gicheru P. 2004. *Soils data derived from SOTER for studies of carbon stocks and change in Kenya (GEF-SOC Project; Version 1.0)*. ISRIC report 2004/01, Wageningen.

Beasley DB, Huggins LF, Monke EJ. 1980. ANSWERS: a model for watershed planning. *Transactions of the ASAE* **23**(4): 938–944.

Burrough PA, McDonnel RA. 1998. *Principles of Geographical Information System*, Oxford University Press: New York.

Callow JN, Van Niel KP, Boggs GS. 2006. How does modifying a DEM to reflect known hydrology affect subsequent terrain analysis? *Journal of Hydrology* **332**: 30–39. DOI: 10.1016/j.jhydrol.2006.06.020.

Carpenter TM, Sperfslage JA, Georgakakos KP, Sweeney T, Fread DL. 1999. National threshold runoff estimation utilizing GIS in support of operational flash flood warning systems. *Journal of Hydrology* **224**: 21–44. DOI: 10.1016/S0022-1694(99)00115-8.

Cerdan O, Le Bissonnais Y, Govers G, Lecomte V, van Oost K, Couturier A, King C, Dureuil N. 2004. Scale effect on runoff from experimental plots to catchments in agricultural areas in Normandy. *Journal of Hydrology* **299**: 4–14. DOI: 10.1016/j.jhydrol.2004.02.017.

Chow VT, Maidment DR, Mays LW. 1988. *Applied Hydrology*, McGraw-Hill: New York.

Congalton RG, Green K. 1999. *Assessing the Accuracy of Remotely Sensed Data*, CRC Press: Boca Raton, Florida.

Coppin P, Jonckheere I, Nackaerts K, Muys B. 2004. Digital change detection methods in ecosystem monitoring: a review. *International Journal of Remote Sensing* **25**: 1565–1596. DOI: 10.1080/0143116031000101675.

Corey JAB, Navjot SS, Kelvin S-HP, Barry WB. 2007. Global evidence that deforestation amplifies flood risk and severity in the developing world. *Global Change Biology* **13**: 2379–2395. DOI: 10.1111/j.1365–2486.2007.01446.x.

Cowan WL. 1956. Estimating hydraulic roughness coefficients. *Agricultural Engineering* **37**(7): 473–475.

Cressie NAC. 1993. *Statistics for Spatial Data*, Wiley: New York.

Cunderlik MJ, Simonovic PS. 2007. Inverse flood risk modelling under changing climatic conditions. *Hydrological Processes* **21**: 563–577. DOI: 10.1002/hyp.6225.

Di Gregorio A, Jansen LJM. 1998. *Land Cover Classification System (LCCS): Classification Concepts and User Manual*, vol. 157. Environment and Natural Resources Service (SDRN): Rome, Italy. DOI: 10.1002/(SICI)1099-1085(199805)12 : 6<843::AID-HYP658>3.0.CO;2-R.

De Jeu RAM, Owe M. 2003. Further validation of a new methodology for surface moisture and vegetation optical depth retrieval. *International Journal of Remote Sensing* **24**(22): 4559–4578. DOI: 10.1080/0143116031000095934.

Doll P, Berkhoff K, Bormann H, Fohrer N, Gerten D, Hagemann S, Krol M. 2008. Advances and visions in large-scale hydrological modelling:

findings from the 11th Workshop on Large-Scale Hydrological Modelling. *Advances in Geosciences* **18**: 51–61.

FAO-UNESCO. 1998. *Soil map of the world, revised legend*. FAO World Soil Resources report number 60, Food and Agricultural Organization of the United Nations, UNESCO: Rome, Italy.

Fisher JB, Tu KP, Baldocchi DD. 2008. Global estimates of the land–atmosphere water flux based on monthly AVHRR and ISLSCP-II data, validated at 16 FLUXNET sites. *Remote Sensing of Environment* **112**: 901–919. DOI: 10.1016/j.rse.2007.06.025.

Githui F, Mutua F, Bauwens W. 2009. Estimating the impacts of land-cover change on runoff using the soil and water assessment tool (SWAT): case study of Nzoia catchment, Kenya. *Hydrological Sciences Journal* **54**(5): 899–908. DOI: 10.1623/hysj.54.5.899.

Grayson R, Blöschl G. 2000. *Spatial Patterns in Catchment Hydrology—Observations and Modelling*, Cambridge University Press: Cambridge, UK.

Gumbricht T, Lindholm H, Akre A, Szczepanek R, Hessling M, McCarthy J. 1997. GIS integrated modelling of a Himalayan landscape. *International Journal of Water Resources Development* **13**(1): 14–23. DOI: 10.1080/07900629749935.

Kundu PM, Chemelil MC, Onyando JO, Gichaba M. 2008. The use of GIS and remote sensing to evaluate the impact of land cover and land use change on discharges in the River Njoro Watershed, Kenya. *Journal of World Association on Soil Water Conservation* **J2**: 109–120.

Legesse D, Vallet-Coulomb C, Gasse F. 2003. Hydrological response of a catchment to climate and land use changes in the tropical Africa. Case study of the Central Ethiopia. *Journal of Hydrology* **275**: 67–85. DOI: 10.1016/S0022-1694(03)00019-2.

Mallick K, Bhattacharya BK, Chaurasia S, Dutta S, Nigam R, Mukherjee J, Banerjee S, Kar G, Rao VUM, Gadgil AS, Parihar JS. 2007. Evapotranspiration using MODIS data and limited ground observations over selected agroecosystems in India. *International Journal of Remote Sensing* **28**(10): 2091–2110. DOI: 10.1080/01431160600935620.

Martz LW, Garbrecht J. 1998. The treatment of flat areas and closed depressions in automated drainage analysis of raster digital elevation models. *Hydrological Processes* **12**: 843–855.

Mati BM, Mutie S, Gadain H, Home P, Mtalo F. 2008. Impacts of land-use/cover changes on the hydrology of the transboundary Mara River, Kenya/Tanzania. *Lakes and Reservoirs: Research and Management* **13**(2): 169–177. DOI: 10.1111/j.1440–1770.2008.00367.x.

McColl C, Aggett G. 2007. Land-use forecasting and hydrological model integration for improved land-use decision support. *Journal of Environment and Management* **84**: 494–512. DOI: 10.1016/j.jenvman.2006.06.023.

Merz R, Blöschl G. 2007. Ereignisbezogene Abflussbeiwerte. In *Hydrologischer Atlas Österreichs, 3. Lieferung. 5·9*, BMLFUW (eds). Bundesministerium für Land- und Forstwirtschaft, Umwelt und Wasserwirtschaft: Wien, Austria. ISBN 3-85437-250-7.

Miller SN, Kepner WG, Mehaffey MH, Hernandez M, Miller RC, Goodrich DC, Devonald K, Heggem DT, Miller WP. 2002. Integrating landscape assessment and hydrologic modeling for land cover change analysis. *Journal of American Water Resources Association* **38**(4): 915–929. DOI: 10.1111/j.1752-1688.2002.tb05534.x.

Moore ID, Grayson RB, Ladson AR. 1991. Digital terrain modeling: a review of hydrological, geomorphological and biological applications. *Hydrological Processes* **5**: 3–30. DOI: 10.1002/hyp.3360050103.

Mutua BM, Klik A. 2007. Predicting daily streamflow in ungauged rural catchments: the case of Masinga catchment, Kenya. *Hydrological Sciences* **52**(2): 292–304.

Olang LO. 2009. *Analysis of land cover change impact on flood events using remote sensing, GIS and hydrological models. A case study of the Nyando River Basin in Kenya*. PhD thesis, University of Natural Resources and Applied Life Sciences, Vienna, Austria.

Onyando JO. 2000. *Rainfall–Runoff Models for Ungauged Catchments in Kenya*, Shaker Verlag: Aachen, Germany.

Onyando JO, Olang LO, Chemelil MC. 2005. Regional analysis of conceptual rainfall-runoff models for runoff simulation in ungauged catchments of Kenya. *Journal of Civil Engineering Research and Practice* **2**(1): 23–37.

Pilgrim DH, Cordery I. 1992. Flood runoff. In *Handbook of Hydrology*, Maidment DR (ed.). McGraw-Hill: New York.

Ponce VM. 1989. *Engineering Hydrology—Principles and Practices*, Prentice-Hall: Upper Saddle River, New Jersey.

Rambaldi G, Muchemi J, Crawhall N, Monaco L. 2007. Through the eyes of Hunter-Gatherer: participatory 3D modelling among Ogiek indigenous peoples in Kenya. *Information Development* **23**(2–3): 113–128.

Reed S, Koren V, Smith M, Zhang Z, Moreda F, Seo D-J. 2004. Overall distributed model intercomparison project results. *Journal of Hydrology* **298**: 27–60. DOI: 10.1016/j.jhydrol.2004.03.031.

Refsgaard JC, Henriksen HJ. 2004. Modelling guidelines—terminology and guiding principles. *Advances in Water Resources* **27**: 71–82. DOI: 10.1016/j.advwatres.2003.08.006.

Refsgaard JC, Knudsen J. 1996. Operational validation and intercomparison of different types of hydrological models. *Water Resources Research* **32**: 2189–2202.

Reuter HI, Nelson A, Jarvis A. 2007. An evaluation of void filling interpolation methods for SRTM data. *International Journal of Geographical Information Science* **21**(9): 983–1008. DOI: 10.1080/13658810601169899.

Sabol GV. 1988. Clark unit hydrograph and r-parameter estimation. *Journal of Hydraulic Engineering* **114**(1): 103–111.

Saghafian B, Farazjoo H, Bozorgy B, Yazdandoost F. 2007. Flood Intensification due to changes in land use. *Water Resources Management (Springer)* **22**: 1051–1067. DOI: 10.1007/s11269-007-9210-z.

Soil Conservation Service. 1986. *National Engineering Handbook, Section 4*, Soil United States Department of Agriculture: Washington, DC.

USACE. 1994. *Flood Runoff Analysis*. Engineering Manual No. 110-2-1417, US Army Corps of Engineers: Washington, DC.

USACE. 2000a. *Hydrologic Modeling System HEC-HMS. Technical Reference Manual*, US Army Corps of Engineers, Hydrologic Engineering Center: Davis, CA.

USACE. 2000b. *Geospatial Hydrologic Modeling Extension HEC-GeoHMS. Technical Reference Manual*, User's manual, Version 1.0. US Army Corps of Engineers, Hydrologic Engineering Center.

Wagener T. 2003. Evaluation of catchment models. *Hydrological Processes* **17**: 3375–3378. DOI: 10.1002/hyp.5158.

Xu C-Y, Singh VP. 2004. Review on regional water resources assessment models under stationary and changing climate. *Water Resources Management* **18**: 591–612.

Yuan F, Sawaya KE, Loeffelholz BC, Bauer ME. 2005. Land cover classification and changes analysis of the twin cities (Minnesota) Metropolitan Area by multitemporal Landsat remote sensing. *Remote Sensing of Environment* **98**: 317–328. DOI: 10.1016/j.rse.2005.08.006.

